BIOMIMETIC ANCHORING SYSTEM FOR SUSTAINED AND LOCALIZED GASTROINTESTINAL DRUG DELIVERY

Joshua A. Levy[2,3,5], Michael A. Straker[2,4,5], Luke A. Beardslee[2], and Reza Ghodssi[1,2,5]*
[1]Department of Electrical and Computer Engineering, [2]Institute for Systems Research,
[3]Department of Materials Science and Engineering, [4]Fischell Department of Bioengineering,
[5]Robert E. Fischell Institute for Biomedical Devices,
University of Maryland, College Park, Maryland, USA

ABSTRACT

We present a novel application of biomimetic spiny microneedles for an anchoring drug deposit (SMAD) enabling long-term localized treatment of lesions within the GI tract. Mechanical characterizations in *ex-vivo* intestinal tissue demonstrate a 22-fold higher anchoring force than traditional conical molded microneedle (MMN) arrays. Additionally, payload diffusion experiments demonstrate that the SMAD can predictably deliver drugs, locally, to a site of interest with comparable performance to MMNs, indicated by strong logarithmic correlation (R^2=0.9773) across SMAD and MMN data. We anticipate this work will permit exploration of localized GI tract drug delivery, facilitating targeted treatment to reduce adverse drug side effects.

KEYWORDS

Drug Delivery, Gastrointestinal Tract, Tissue Anchoring, Direct Laser Writing

INTRODUCTION

Gastrointestinal (GI) disorders are currently managed by systemic oral and intravenous administration of drugs, resulting in broad dispersal of the therapeutic agents throughout the body [1]. Many therapeutics for gastrointestinal disorders, like immune modulating agents and corticosteroids, are accompanied by adverse side effects that are a consequence of high levels of systemic drug absorption [1], [2]. When delivering these therapeutics systemically, excess agent is required to achieve adequate treatment at sites of interest. Targeted treatment, achieved by delivery to specific locations in the GI tract, could offer comparable remediation of inflammatory sites without the use of excess therapeutic agent. This targeted delivery method serves to reduce side effects related to common GI drugs and lessen excess drug usage and, consequently, drug costs.

A variety of technologies currently exist to increase the regional specificity of drug delivery in the GI tract. Notably, pH-sensitive tablet coatings enable region-specific (stomach, small intestine, etc.) release of the encapsulated therapeutic agents. Additionally, mucoadhesive coatings can be leveraged to slow the transit of a tablet by attaching to mucus-lined tissue; thus, promoting focused release in a target region of the GI tract [2]. However, these technologies only enable broad regional targeting of drug delivery, making it impossible to direct treatment to specific locations in the GI tract. Though helpful, these technologies fail to address the need for location-specific delivery of therapeutic agents.

Enhanced regional targeting has also been achieved using ingestible devices. Although intended for different applications, great focus has been placed recently on ingestible devices for delivery of biological macromolecules such as insulin. Traverso et al. have previously demonstrated a microneedle device for delivery of insulin in the small intestine, controlled by dissolution of a pH-responsive polymer [3]. Abramson et al. demonstrated a self-orienting mm-scale applicator (SOMA) for insulin delivery in the stomach [4], as well as a luminal unfolding microneedle injector (LUMI), for biologic delivery in the small intestine [5]. These microsystems advancements empower site-specific delivery; however, the devices still operate using a broad region-targeting approach.

Targeted and moderately localized delivery has been achieved using fluid release capsule mechanisms. Multiple systems have been developed that use MEMS actuators for site-specific fluid drug delivery [6]–[9]. Additionally, magnetic locomotion and localization systems have been used to facilitate delivery of therapeutics at specific locations in the GI tract. Dietzel et al. utilized a magnetic localization and fluid drug release device to control the location of drug release [10]. However, the precision of drug localization is limited in these systems due to the fluid spread that occurs after drug release. Lee et al. utilized a similar magnetic actuation concept to apply dissolving drug-loaded microneedle patches to the small intestine mucosa to achieve location specific treatment [11]. Although the demonstrated ingestible capsule device showed successful delivery in *ex-vivo* tissue, the authors noted challenges with adhesion of the dissolving molded microneedles (MMNs) to the tissue, inhibiting the potential for prolonged delivery of therapeutics *in-vivo*.

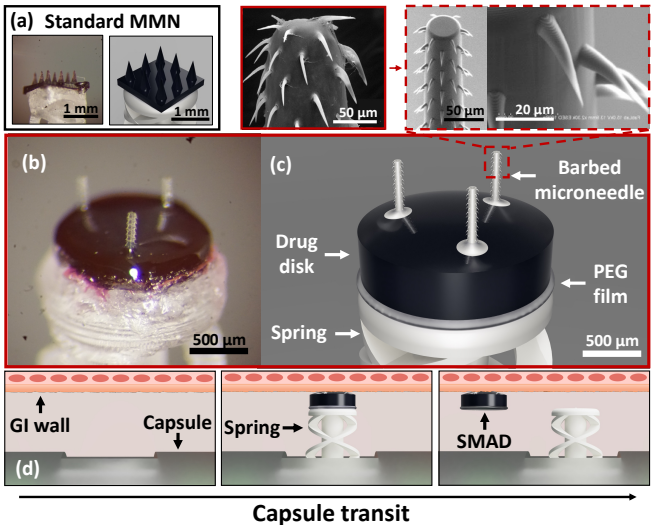

Figure 1: (a) Image and rendering of a standard 3x3 conical molded microneedle (MMN) array attached to the thermomechanical spring actuator and (b) image of SMAD attached to spring actuator. (c) Schematic overview of novel hybrid fabricated SMAD attached to actuator using water-soluble polyethylene glycol (PEG). Three barbed microneedles are attached to the drug disk using epoxy adhesive. (inset, left) Spiny headed worm proboscis from [12] and (inset, right) SEM image of biomimetic anchoring microneedle from [13]. (d) Spring actuator fires on command during capsule transit through the small intestine. The SMAD is anchored in the mucosal tissue by the barbed microneedles, leaving the deposit in the tissue to release the loaded drug by diffusion.

978-1-940470-04-7/HH2022/$25©2022TRF
DOI 10.31438/trf.hh2022.22

To address the need for a reliable mechanism capable of highly localized and sustained therapeutic delivery, we demonstrate the application of biomimetic spiny microneedles, previously developed in our group [13], as an anchor for a dissolving drug deposit (Fig. 1). The spiny microneedles in this system are attached to a solvent-cast water-soluble drug disk that distributes therapeutic agent through a diffusion process. The system is designed to complement a previously demonstrated thermomechanical spring actuator [14] and is mechanically removed from this actuator after anchoring to the GI mucosa. Characterization of the system showed greatly increased anchoring capabilities of the SMAD when compared to traditional molded microneedles — signifying both improved tissue adherence and system reliability. The SMAD also demonstrates the ability to deliver model drug as efficiently as penetrating MMNs in an agarose medium.

EXPERIMENTAL METHODS

SMADs were fabricated by a hybrid process merging direct laser writing (DLW) of the barbed microneedles presented in [13] and solvent casting of model drug disks (∅=2 mm, t=500 µm) from 20 %w/v polyvinyl alcohol (PVA) containing FD&C Blue #1.

DLW of Barbed Microneedles

Barbed microneedles were fabricated by DLW using a similar protocol to that previously demonstrated in our group by Liu et al. [13]. The microneedles are 650 µm in height with a 74 µm tip diameter and a 300 µm flared base for enhanced adhesion to the drug disk. Each needle contains a total of 72 backward-facing barbs with high sharpness (~1 µm) that promote robust tissue anchoring. DLW was performed using the Dip-in Laser Lithography (DiLL) mode on a fused silica substrate with the Nanoscribe Photonic Professional GT (Nanoscribe GmbH, Karlsruhe, Germany). Biocompatible (ISO-10993-5) IP-S photoresist was used with a 25x objective and a slicing distance of 1 µm to fabricate a 3-needle array. Needles were printed upside down in a triangular pattern, supporting reliable attachment to the drug disk and control over the spatial arrangement of the needles on the fabricated structure. Post print, needle arrays were cleaned in propylene glycol monomethyl ether acetate (PGMEA) for 15 min, followed by 5 min in isopropyl alcohol.

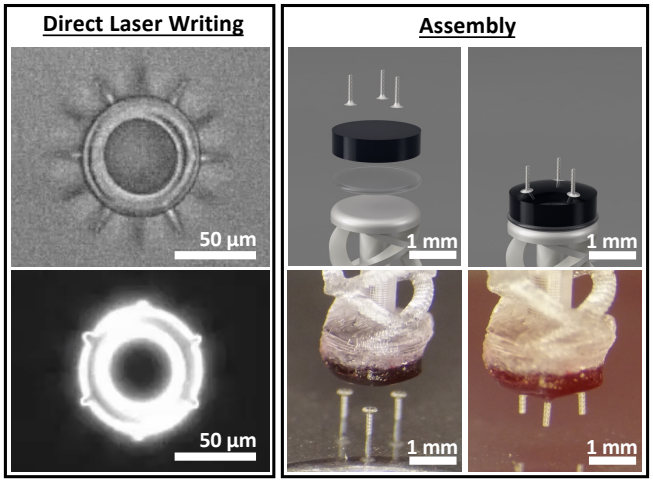

Figure 2: (left) DiLL mode DLW of barbed microneedle using Nanoscribe (NA=0.8). (right) Assembly of drug deposit structure by PEG attachment of the drug disk to the spring actuator then adhesion of the spiny microneedles using Loctite M-21HP biocompatible (ISO-10993) medical device epoxy adhesive.

Solvent Casting of Model Drug Disk

Model drug disks are fabricated by solvent casting a film containing 20 %w/v PVA (MW 31-50 kDa) (Sigma Aldrich, St. Louis, MO, USA) with FD&C blue #1 dye to visualize drug diffusion. The solvent is allowed to evaporate for 24 h, then drug disks (∅=2 mm) are punched from the resultant film.

Assembly of SMAD

Drug disks are first attached to the previously demonstrated spring actuator [14] with ~1.5 µg of melted polyethylene glycol (PEG). As can be seen in Fig. 2, the disk is then lowered onto the flared bases of the 3-microneedle array and adhered using Loctite M-21HP biocompatible (ISO-10993) epoxy adhesive (Henkel Corporation, Stamford, CT, USA). After 4 h is allowed for the epoxy resin to cure, the SMAD assembly is retracted, detaching the barbed microneedles from the fused silica substrate.

Solvent Casting of Conical Molded Microneedles

MMNs were fabricated by solvent casting PVA containing FD&C blue #1 dye, an identical composition to the solution used for solvent casting of model drug disks. Polydimethylsiloxane (PDMS) microneedle molds were acquired from Blueacre Technology Ltd. (Dundalk, Co Louth, Ireland). The microneedle mold has a 11x11 array of 600 µm needles with a base diameter of 300 µm, and an interspacing of 600 µm on center. 500 µL of the PVA solution was deposited on the needle array mold, then placed under vacuum for 15 min to remove air from the needle mold voids. The solvent was allowed to evaporate for 24 h, then a 3x3 needle array was cut from the molded part. The 3x3 array was then attached to the spring actuator using 1.5 µg of melted PEG.

Mechanical Anchoring and Removal Testing

Mechanical tests were performed to compare SMAD and MMN tissue anchoring and removal forces. This was done using an Instron 5942 universal test apparatus (Instron Corporation, Norwood, MA, USA) equipped with a 50 N load cell. All tests were performed using a crosshead speed of 1 mm/min. Spring actuators fitted with MMN or SMAD tip structures were lowered onto tissue samples until reaching the previously reported actuator force of 75 mN [14]. Tissue samples were pre-coated with a ~2 mm layer of 1X PBS (Sigma Aldrich, St. Louis, MO, USA) to simulate the presence of mucus and aqueous intestinal media on the tissue surface. Upon reaching the 75 mN force, the tissue was moved 2 mm laterally to imitate the longitudinal motion experienced in the GI tract. The sample is then retracted, resulting in the detachment or sustained attachment of the respective tip structures. Detachment or removal force was measured for each sample to determine the strength of the tip structure attachment when compared to the anchoring force for each type of tip structure. Tip detachment force was determined as the removal force of the SMAD from the actuator.

Model Drug Delivery

Dye-loaded SMAD (n=5) and MMN (n=5) samples were applied to a thin agarose surface and dye diffusion was tracked at predetermined time intervals from 0 to 168 h. Images of each sample were captured at each time point in a light-controlled environment, enabling a quantitative image analysis approach for data interpretation using MATLAB R2021b (MathWorks Corporation, Natick, MA, USA). From each image, the red color channel was isolated, and the resultant grayscale was binarized with a threshold intensity of 40 %. The resulting binary matrix was used to determine the areal dye spread and diffusion radius as a function of time. After 168 hr, the agarose samples were submerged in DI water to allow the dye to be diluted to within the linear regime of optical density.

Optical density of diluted samples was then obtained using a Molecular Devices SpectraMax Plus spectrophotometer (San Jose, CA, USA). Optical density measurements were compared to a calibration curve to determine the initial dye mass for each sample. These values are used to account for concentration-related differences in diffusion behavior, enabling a more pertinent comparison of model drug delivery.

RESULTS AND DISCUSSION

The SMAD was evaluated qualitatively by lateral removal experiments to imitate the longitudinal motion of a capsule in the GI tract. Performance of the SMAD was then quantitatively compared to that of a 3x3 MMN array, looking at mechanical removal and anchoring properties as well as the dynamics of drug delivery from each structure.

Removal by Lateral Translation

A capsule in the GI tract will experience periodic peristaltic movements; thus, a significant component of force will be applied perpendicular to the actuation direction. To model this, the SMAD was attached to an actuator and translated laterally (Fig. 3) until the SMAD structure was removed. Removal occurs at approximately 3 mm deflection, corresponding to 3 mm of capsule transit within the intestine.

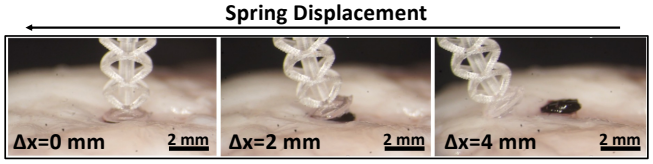

Figure 3: Tissue anchoring and deposit removal upon ca. 3 mm lateral deflection of the spring actuator. Lateral motion is intended to simulate capsule transit through the GIT.

Mechanical Characterization of Tissue Anchoring

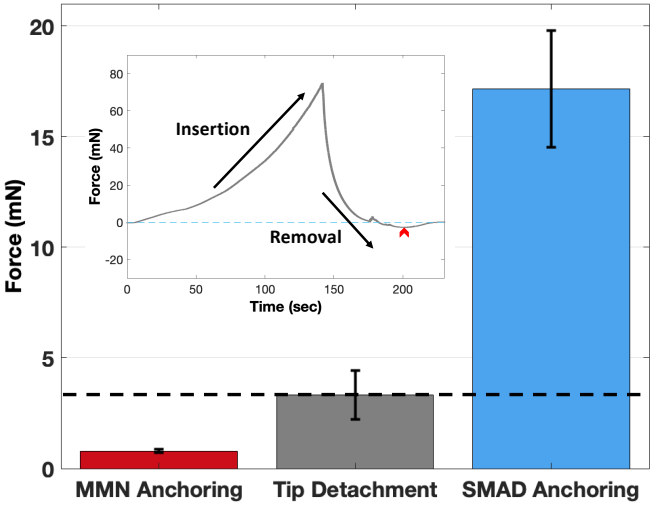

Figure 4: SMAD anchoring force (17.2 mN) exceeds required detachment force (3.3 mN) while MMN anchoring force (0.8 mN) is insufficient. Dashed line indicates detachment force threshold. Error bars represent standard error (n=4). Inset: Force loading throughout insertion and removal. Red arrow indicates tip detachment force.

Firm tissue anchoring is critical for removal of the SMAD from the actuator, but it also enables robust adherence to the target region and, consequently, reliable prolonged therapeutic delivery. Fig. 4 shows mechanical removal and tip detachment data of the SMAD compared to MMNs. 'Tip detachment force' refers to removal force of the SMAD or MMN structure from atop the actuator, while 'anchoring force' refers to the force required to remove the SMAD or MMN structure from the tissue sample. The conical MMNs showed a low anchoring force of 0.8±0.1 mN compared to the 3.3±1.1 mN force required to detach the tip structure from the actuator. Conversely, the SMAD demonstrated an anchoring force of 17.2±2.6 mN, a 22-fold improvement over the conical MMNs and significantly higher than the detachment force. The exceptional anchoring ability of the structure compared to the MMNs affects more reliable tissue anchoring and system operation. The inset in Fig. 4 illustrates the force loading and unloading during experimentation, including a red arrow indicating the point of detachment or removal.

Model Drug Delivery

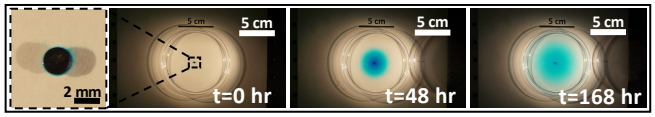

Figure 5: Diffusion of dye from drug disk at selected time points over 168 hr. Illumination is controlled across all samples to mitigate error in the image processing used to determine radius of diffusion.

Fig. 5 shows the release and subsequent diffusion of dye from a SMAD sample at 0 hr, 48 hr, and 168 hr. At 48 hr, the visually discernable perimeter of dye diffusion is at a radial distance of ~1.8 cm, while this expands to ~2.5 cm after 168 hr. 5 samples of each SMAD and MMN were characterized using this diffusion approach, as represented quantitatively in Fig. 6.

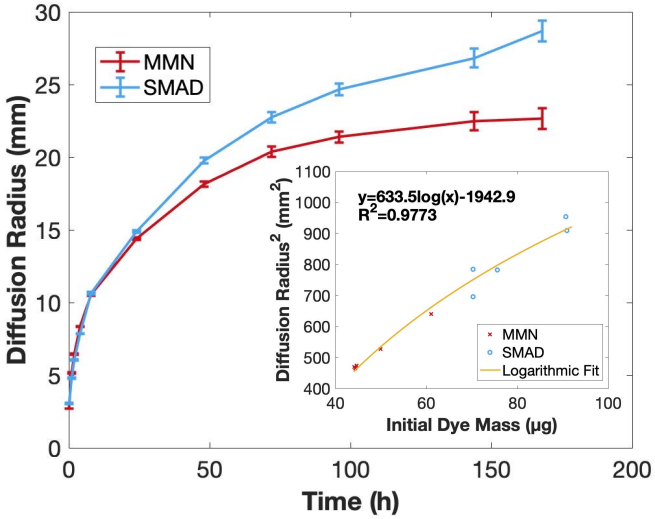

Figure 6: Diffusion profile of SMAD and MMN up to 168 hr. Error bars indicate standard error (n=5). Inset: Final squared diffusion radius (t=168 hr) shows a logarithmic correlation to initial dye mass (R^2=0.9773) predicted by the solution to Fick's second law for radial diffusion distance. The logarithmic fit coefficient predicts a diffusion constant of $D=2.6 \times 10^{-10}$ m^2/s that agrees strongly with previously reported value ($D= (2.5 \pm 0.2) \times 10^{-10}$ m^2/s) for dye diffusion in agar gel [15] confirming the relevance of the calculated logarithmic correlation coefficient.

Fig. 6 shows the mean diffusion radius at each measured time point for the SMAD and MMN. By initial observation, there exists a discrepancy between the extent of diffusion from the MMN and

SMAD. However, a difference in outcomes can be expected due to variations in initial dye mass between MMN and SMAD structures.

The thin agarose diffusion medium constrains diffusion to two dimensions; thus, this case most closely resembles 2D Fickian diffusion. The time-dependent concentration profile pertaining to this diffusion case is described by equation 1, where C is concentration, C_0 is initial concentration, D is the diffusion constant in the given medium, t is time, and r is radial distance.

$$C=C_0 \frac{1}{\sqrt{4\pi Dt}} e^{-\frac{r^2}{4Dt}} \quad (1)$$

The extent of diffusion from each sample can be measured by the radial diffusion distance at which the dye concentration exceeds a threshold value. With consistent lighting, the threshold concentration value corresponds to a constant light intensity value in the dye spreading image. Thus, the red channel light intensity with blue dye can be used as a direct indicator of the local dye concentration — enabling a quantitative treatment of the diffusion to account for differences in initial dye content across samples. For a given intensity threshold (T) solving for the thresholded squared radial diffusion distance (r^2) yields equation 2.

$$r^2=4Dt\left(ln(C_0) - ln\left(2T(\pi Dt)^{\frac{1}{2}}\right)\right) \quad (2)$$

At a specific measurement time, D, t, and T are constant and r^2 carries a logarithmic dependence on the initial concentration; therefore, one time point can be used to compare the relationship between r^2 and C_0 for the SMAD and MMN cases. The inset in Fig. 6 uses t=168 hr to compare the radial diffusion distance with initial dye mass in the context of equation 2. The data, across both groups, obeys the equation with R^2=0.9773. To validate the logarithmic character, a diffusion coefficient of $D=2.6\times10^{-10}$ m^2/s was calculated from the logarithmic coefficient using equation 2. This value is in strong agreement with previously reported values for the diffusion of dye in agar gel ($D= (2.5 \pm 0.2) \times 10^{-10}$ m^2/s) [15], corroborating the logarithmic data trend.

CONCLUSION

In this paper we introduce the first application of biomimetic barbed microneedles toward drug delivery in the GI tract. This is accomplished by a spiny microneedle anchoring deposit (SMAD) structure, composed of the spiny microneedles attached to a dissolving drug loaded PVA deposit. The high resolution (~1 μm) of the DLW process enables high sharpness and firm tissue anchoring. SMADs with the barbed microneedles anchored with a 22-fold higher tissue retention force than conical molded microneedles — reliably overcoming the force required for removal of the SMAD from the spring actuator. SMADs also demonstrated comparable drug delivery characteristics to the standard MMNs through model drug delivery in an agarose medium. After correction for the initial dye mass in each sample, the SMAD and MMN data showed high correlation (R^2=0.9773) indicating predictable and comparable performance. Overall, the robust anchoring provided by this system will enable location-specific and long-term anchoring of a drug deposit to facilitate prolonged treatment of target locations in the GI tract, opening new possibilities for therapeutic treatment of GI diseases.

ACKNOWLEDGEMENTS

This work was supported by the National Science Foundation ECCS Program under Award #1939236. The authors acknowledge support from the Clark Doctoral Fellows Program, TerrapinWorks, the University of Maryland NanoCenter and its FabLab.

REFERENCES

[1] K. E. Trinkley and M. C. Nahata, "Treatment of irritable bowel syndrome," *Journal of Clinical Pharmacy and Therapeutics*, 36, 3 (2011).

[2] S. Hua, "Advances in Oral Drug Delivery for Regional Targeting in the Gastrointestinal Tract - Influence of Physiological, Pathophysiological and Pharmaceutical Factors," *Frontiers in Pharmacology*, 11 (2020).

[3] G. Traverso, C.M Schoellhammer, A Schroeder, R. Maa, G.Y Lauwers, B.E. Polat, D.G. Anderson, D. Blankschtein, R. Langer, "Microneedles for Drug Delivery via the Gastrointestinal Tract," *J Pharm Sci*, 104, 2 (2015).

[4] A. Abramson, E. Caffarel-Slavador, M. Khang, A. Vegge, F. Hubalek, *et al.*, "An ingestible self-orienting system for oral delivery of macromolecules," *Science*, 363, 6427 (2019).

[5] A. Abramson *et al.*, "A luminal unfolding microneedle injector for oral delivery of macromolecules," *Nature Medicine*, 25, 10 (2019).

[6] P. Xitian, L. Hongying, W. Kang, L. Yulin, Z. Xiaolin, and W. Zhiyu, "A novel remote controlled capsule for site-specific drug delivery in human GI tract," *International Journal of Pharmaceutics*, 382, 1–2 (2009).

[7] X. Pi *et al.*, "A novel micro-fabricated thruster for drug release in remote controlled capsule," *Sensors and Actuators A: Physical*, 159, 2 (2010).

[8] J. Cui, X. Zheng, W. Hou, Y. P. Zhuang, X. Pi, and J. Yang, "The study of a remote-controlled gastrointestinal drug delivery and sampling system," *Telemedicine and e-Health*, 14, 7 (2008).

[9] L. Hongying, X. Pi, C. Zhou, X. Zheng, W. Hou, and Z. Wen, "Design of site specific delivery capsule based on MEMS," *3rd IEEE International Conference on Nano/Micro Engineered and Molecular Systems, NEMS* (2008)

[10] C. T. Dietzel, H. Richert, S. Abert, U. Merkel, M. Hippius, and A. Stallmach, "Magnetic Active Agent Release System (MAARS): Evaluation of a new way for a reproducible, externally controlled drug release into the small intestine," *Journal of Controlled Release*, 161, 3 (2012).

[11] J. Lee, H. Lee, S. hyun Kwon, and S. Park, "Active delivery of multi-layer drug-loaded microneedle patches using magnetically driven capsule," *Medical Engineering & Physics*, 85 (2020).

[12] O. M. Amin, R. A. Heckmann, and N. van Ha, "Acanthocephalans from fishes and amphibians in Vietnam, with descriptions of five new species," *Parasite*, 21 (2014).

[13] S. Liu, S. Chu, G. E. Banis, L. A. Beardslee, and R. Ghodssi, "Biomimetic Barbed Microneedles for Highly Robust Tissue Anchoring," *Proceedings of the IEEE International Conference on Micro Electro Mechanical Systems (MEMS)* (2020).

[14] J.A. Levy, J.M. Stine, L.A. Beardslee, and R. Ghodssi, "Thermally Released Spring-Loaded Platform for Capsule Based Drug Delivery and Sensing.," *67th AVS Symposium & Exhibit*. Virtual (2021).

[15] A. Simonsen, A. Røyset, L. O. Svaasand, O. J. Løkberg, T. Lindmo, and T. Støren, "Measurement of dye diffusion in agar gel by use of low-coherence interferometry," *Optics Letters, 28, 14* (2003).

CONTACT

*R. Ghodssi, tel: +1-301-405-8158; ghodssi@umd.edu